Journal of *Fungi*

MDPI

Article

Cytochalasans from the Endophytic Fungus *Phomopsis* sp. shj2 and Their Antimigratory Activities

Bing-Chao Yan [1,2,3], Wei-Guang Wang [1,2], Ling-Mei Kong [1,2], Jian-Wei Tang [1,2,3], Xue Du [1,2,3], Yan Li [1,2] and Pema-Tenzin Puno [1,2,3,*]

[1] State Key Laboratory of Phytochemistry and Plant Resources in West China, Kunming Institute of Botany, Chinese Academy of Sciences, Kunming 650201, China; yanbingchao@mail.kib.ac.cn (B.-C.Y.); wwg@live.cn (W.-G.W.); konglingmei@mail.kib.ac.cn (L.-M.K.); tangjianwei@mail.kib.ac.cn (J.-W.T.); duxue@mail.kib.ac.cn (X.D.); liyan@mail.kib.ac.cn (Y.L.)
[2] Yunnan Key Laboratory of Natural Medicinal Chemistry, Kunming 650201, China
[3] University of Chinese Academy of Sciences, Beijing 100049, China
* Correspondence: punopematenzin@mail.kib.ac.cn

Abstract: Cytochalasans from the endophytic fungi featured structure diversity. Our previous study has disclosed that cytochalasans from the endophytic fungus *Phomopsis* sp. shj2 exhibited an antimigratory effect. Further chemical investigation on *Phomopsis* sp. shj2 has led to the discovery of seven new cytochalasans (**1**–**7**), together with four known ones. Their structures were elucidated through extensive spectroscopic data interpretation and single-crystal X-ray diffraction analysis. Compounds **1**–**3** and **8**–**11** exhibited antimigratory effects against MDA-MB-231 in vitro with IC_{50} values in the range of 1.01−10.42 μM.

Keywords: endophytic fungus; *Phomopsis*; cytochalasan; antimigratory activity

check for updates

Citation: Yan, B.-C.; Wang, W.-G.; Kong, L.-M.; Tang, J.-W.; Du, X.; Li, Y.; Puno, P.-T. Cytochalasans from the Endophytic Fungus *Phomopsis* sp. shj2 and Their Antimigratory Activities. *J. Fungi* **2022**, *8*, 543. https://doi.org/10.3390/jof8050543

Academic Editors: Tao Feng and Frank Surup

Received: 1 May 2022
Accepted: 20 May 2022
Published: 23 May 2022

1. Introduction

Endophytic fungi are emerging as rich resources for structurally unique and bioactive secondary metabolites, which arouse increasing research interest in the past decades [1–3]. Cytochalasans represent a large class of fungal polyketide synthase-nonribosomal peptide synthetase (PKS-NRPS) hybrid secondary metabolites. Recently, plenty of polycyclic cytochalasans have been identified [4–8] and synthesised [9,10]; moreover, they exhibited a broad spectrum of interesting biological activities, such as cytotoxic [4,5,8], immunoregulatory [11], and antimicrobial [6] activities. To date, more than 400 cytochalasans have been isolated from various fungal sources, such as *Phomopsis* [4], *Xylaria* [12], *Chaetomium* [13] and *Phoma* [14] genera.

Tumour spread is a major concern in cancer therapeutics as cancer metastasis is responsible for 90% of deaths from solid tumours [15]. Natural products with antimigratory activity represent a highly interesting field to explore for cancer chemoprevention and therapy. Fungi are emerging as a natural source, such as *Diaporthe* [16], *Isaria* [17], and *Phenicillium* [18,19] genera. Chemical investigations on endophytes of *Isodon* species have disclosed structurally diverse and bioactive natural products [19–22]. Phomopchalasins B and C were isolated from the endophytic fungus *Phomopsis* sp. shj2 from the stems of *Isodon eriocalyx* var. *laxiflora* and exhibited in vitro antimigratory effects against MDA-MB231 [19]. In our continuous efforts for more bioactive structures, the strain was further investigated by one strain-many compounds strategy (OSMAC), which led to the isolation of seven new cytochalasans (**1**–**7**), along with four known ones (Figure 1). Herein, we report the isolation, structure elucidation, and antimigratory activities of these cytochalasans.

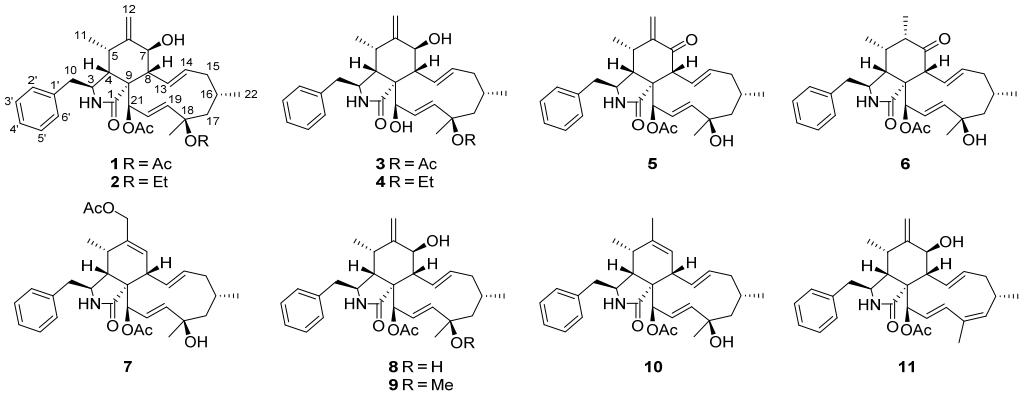

Figure 1. Structures of compounds **1**–**11**.

2. Materials and Methods

2.1. General Experimental Procedures

Column chromatography (CC) was performed with silica gel (100–200 mesh, Qingdao Marine Chemical, Inc., Qingdao, China), Lichroprep RP-18 gel (40–63 μm, Merck, Darmstadt, Germany). Preparative HPLC and semi-preparative HPLC were performed on an Agilent 1200 liquid chromatograph with a Zorbax SB-C18 (9.4 mm × 25 cm) column. Fractions were monitored by TLC, and spots were visualized by heating silica gel plates sprayed with 10% H_2SO_4 in EtOH. Petroleum ether (PE, 60–90 °C), EtOAc, $CHCl_3$, acetone, MeOH, and EtOH were of analytical grade and purchased from Sinopharm Chemical Reagent Co. Ltd., China. All solvents were distilled before use. NMR spectra were recorded on Bruker DRX-500, AV-600, and 800 spectrometers. ESIMS and HRESIMS experiments were performed on a Bruker HCT/Esquire spectrometer and a Waters AutoSpec Premier P776 spectrometer. CD spectra were measured on an Applied Photophysics Chirascan spectrophotometer. Optical rotations were measured with a JASCO P-1020 polarimeter. UV spectra were obtained using a Shimadzu UV-2401A spectrophotometer.

2.2. Fungal Material

The culture of *Phomopsis* sp. shj2 was isolated from the stems of *Isodon eriocalyx* var. *laxiflora* collected from Kunming Botanical Garden, Kunming, People's Republic of China, in December 2012. The isolate was identified based on sequence (GenBank Accession No. KU533636) analysis of the ITS region of the rDNA. The fungal strain was cultured on slants of potato dextrose agar at 25 °C for 7 days. Agar plugs were cut into small pieces (about 0.5 × 0.5 × 0.5 cm^3) under aseptic conditions, and 15 pieces were used to inoculate three Erlenmeyer flasks (250 mL), each containing 50 mL of media (0.4% glucose, 1% malt extract, and 0.4% yeast extract); the final pH of the media was adjusted to 6.5, and the flasks were sterilized by autoclave. Three flasks of the inoculated media were incubated at 28 °C on a rotary shaker at 180 rpm for 5 days to prepare the seed culture. Fermentation was carried out in 125 Fernbach flasks (500 mL), each containing 80 g of rice. Spore inoculum was prepared in sterile, distilled H_2O to give a final spore/cell suspension of 1 × 10^6/mL. Distilled H_2O (120 mL) was added to each flask, and the contents were soaked overnight before autoclaving at 15 psi for 30 min. After cooling to room temperature, each flask was inoculated with 5.0 mL of the spore inoculum and incubated at 28 °C for 42 days.

2.3. Extraction and Isolation

The fermented material was extracted with EtOAc (4 × 10.0 L) and the organic solvent was evaporated to dryness under vacuum to afford a crude extract (170 g). The crude extract was purified by CC (column chromatography on SiO_2 with $CHCl_3$/acetone gradient system 1:0, 9:1, 8:2, 7:3, 6:4 and 1:1) to yield six main fractions, Fr.s A–F. Fr. B was subjected to chromatography over silica gel CC (petroleum ether-EtOAc) to give subfractions B1–B9. Fr. B2 was further purified by silica gel CC (petroleum ether-acetone) to give **1** (10.7 mg).

Fr. B8 was purified by semi-preparative HPLC (3 mL/min, detector UV λ_{max} 210 nm, MeCN-H_2O) to afford **11** (3.2 mg), **8** (25.1 mg), and **10** (3.7 mg). Fr. C was purified by chromatography over silica gel CC (petroleum ether-acetone) to give subfractions Fr.s C1–C10. The subfraction C8 was recrystallized to give **7** (20.5 mg). Fr. C5 was separated by semi-preparative HPLC (3 mL/min, detector UV λ_{max} 210 nm, MeCN-H_2O) to afford **3** (4.7 mg) and **9** (10.2 mg). Fr. D was subjected to Sephadex LH-20 (CH_3Cl-MeOH) to yield subfractions D1–D6. The subfraction D5 was purified by recrystallization to afford **4** (1.2 mg). And Fr. D5 was further purified to afford **2** (20.3 mg). Fr. E was purified by semi-preparative HPLC (3 mL/min, detector UV λ_{max} 210 nm, MeCN-H_2O) to afford **5** (1.5 mg) and **6** (1.6 mg).

18-Acetoxycytochalasin H (**1**): white powder (MeOH); $[\alpha]_D^{20}$ = +44.2 (c 0.23, MeOH), UV (MeOH) λ_{max} (log ε): 203.2 (0.5151); ^1H and ^{13}C NMR data, see Tables 1 and 2; HRESIMS $[M + Na]^+$ m/z 558.2826 (calcd for $C_{32}H_{41}NO_6Na$, 558.2826).

Table 1. ^1H NMR data ($CDCl_3$, δ in ppm) of compounds **1**–**7**.

No.	1 [a,b]	2 [a,c]	3 [c,d]	4 [a,c]	5 [a,c]	6 [a,e]	7 [a,c]
3	3.25 (m)	3.26 (m)	3.33 (m)	3.27 (m)	3.23 (dt, 9.4, 4.3)	3.54 (dt, *J* = 9.4, 4.3)	3.28 (overlap)
4	2.15 (m)	2.14 (m)	2.65 (m)	2.58 (m)	2.35 (t, 4.3)	2.25 (t, 4.2)	2.19 (t, 4.3)
5	2.76 (m)	2.78 (m)	2.72 (m)	2.90 (m)	3.08 (m)	2.11 (m)	2.53 (m)
6						2.01 (m)	
7	3.84 (d, 10.5)	3.83 (d, 10.5)	3.79 (d, 10.5)	3.82 (d, 10.5)			5.72 (s)
8	2.93 (d, 10.5)	2.96 (d, 10.5)	2.94 (d, 10.5)	2.90 (d, 10.5)	3.94 (d, 9.3)	3.79 (d, 9.4)	3.26 (overlap)
10	2.85 (dd, 13.5, 4.5) 2.65 (dd, 13.5, 9.6)	2.86 (dd, 13.3, 3.8) 2.67 (m)	2.81 (m) 2.79 (m)	2.58 (m) 1.71 (m)	2.90 (dd, 13.5, 4.3) 2.65 (dd, 13.5, 9.4)	2.92 (dd, 13.5, 4.3) 2.64 (dd, 13.5, 9.4)	2.91 (dd, 13.5, 4.3) 2.60 (dd, 13.5, 10.2)
11	0.99 (d, 6.7)	1.01 (d, 6.7)	0.84 (d, 6.8)	1.10 (d, 6.7)	1.12 (d, 6.7)	0.98 (d, 6.7)	1.17 (d, 7.3)
12	5.33 (s) 5.10 (s)	5.35 (s) 5.11 (s)	5.18 (s) 4.95 (s)	5.32 (s) 5.11 (s)	6.25 (s) 5.29 (s)	1.12 (d, 7.0)	4.53 (d, 12.8) 4.48 (d, 12.8)
13	5.74 (dd, 15.5, 9.7)	5.73 (dd, 15.1, 10.0)	5.70 (dd, 15.0, 9.2)	5.71 (dd, 15.5, 9.8)	5.81 (dd, 15.6, 9.3)	5.69 (dd, 15.5, 9.4)	5.84 (dd, 15.3, 10.3)
14	5.38 (m)	5.43 (m)	5.22 (m)	5.35 (m)	5.19 (m)	5.16 (m)	5.24 (m)
15	2.01 (overlap) 1.79 (d, 12.4)	2.00 (overlap) 1.79 (d, 11.3)	1.90 (dd, 13.9, 3.1) 1.80 (m)	1.98 (dd, 10.4, 4.7) 1.78 (m)	2.04 (dd, 12.9, 4.4) 1.89 (m)	2.01 (m) 1.81 (m)	1.99 (m) 1.77 (overlap)
16	1.65 (m)	1.78 (m)	1.66 (m)	1.75 (m)	1.76 (m)	1.75 (m)	1.75 (m)
17	2.05 (dd, 14.3, 3.7), 1.75 (dd, 14.3, 3.0	1.69 (m)	1.90 (m) 1.75 (m)	1.78 (overlap)	1.85 (overlap) 1.54 (dd, 14.3, 3.2)	1.85 (m) 1.53 (dd, 14.3, 3.1)	1.88 (dd, 14.3, 2.7) 1.54 (d, 14.3)
19	5.56 (d, 16.6)	5.52 (d, 16.7)	5.84 (d, 16.7)	5.73 (d, 16.7)	5.52 (d, 16.6)	5.49 (d, 16.6)	5.52 (d, 16.6)
20	5.85 (dd, 16.6, 2.3)	5.79 (dd, 16.7, 2.4)	5.97 (dd, 16.7, 2.2)	5.99 (dd, 16.7, 2.6)	5.90 (dd, 16.6, 2.6)	5.85 (dd, 16.6, 2.5)	5.91 (dd, 16.6, 2.6)
21	5.63 (t, 2.3)	5.54 (t, 2.4)	4.02 (t, 2.2)	4.12 (t, 2.6)	5.65 (t, 2.6)	5.60 (t, 2.5)	5.68 (t, 2.6)
22	1.02 (d, 6.9)	1.01 (d, 6.5)	0.99 (d, 6.3)	1.01 (d, 6.3)	1.04 (d, 7.0)	1.03 (d, 6.9)	1.04 (d, 6.3)
23	1.58 (s)	1.26 (s)	1.53 (s)	1.28 (s)	1.34 (s)	1.32 (s)	1.34 (s)
2′, 6′	7.14 (d, 7.4)	7.15 (d, 7.4)	7.21 (d, 7.3)	7.15 (d, 7.4)	7.12 (d, 7.4)	7.15 (d, 7.3)	7.14 (d, 7.2)
3′, 5′	7.31 (t, 7.4)	7.32 (t, 7.4)	7.29 (t, 7.3)	7.31 (t, 7.4)	7.32 (t, 7.4)	7.33 (t, 7.3)	7.31 (t, 7.5)
4′	7.25 (t, 7.4)	7.25 (t, 7.4)	7.26 (d, 7.3)	7.24 (t, 7.4)	7.25 (t, 7.4)	7.25 (t, 7.3)	7.24 (t, 7.2)
12-OAc							2.04, s
18-OR	R = Ac 2.00 (s)	R = Et 3.38 (m), 2.65 (m) 1.14 (t, 6.9)	R = Ac 1.96 (s)	R = Et 3.41 (m), 3.37 (m) 1.17 (t, 7.0)	R = H	R = H	R = H
21-OAc	2.24 (s)	2.25 (s)			2.30 (s)	2.28 (s)	2.25 (s)

[a] Recorded in $CDCl_3$. [b] Recorded at 800 MHz. [c] Recorded at 600 MHz. [d] Recorded in acetone-d_6. [e] Recorded at 500 MHz.

Table 2. ^{13}C NMR data ($CDCl_3$, δ in ppm) of compounds **1**–**7**.

No.	1 [a,b]	2 [a,c]	3 [d,e]	4 [a,e]	5 [a,e]	6 [a,f]	7 [a,e]
1	174.3 s	174.3 s	176.7 s	175.8 s	172.8 s	173.5 s	174.9 s
3	53.9 d	53.9 d	54.2 d	50.6 d	54.0 d	53.3 d	56.1 d
4	50.5 d	50.9 d	50.2 d	53.9 d	50.6 d	51.1 d	53.8 d
5	33.0 d	33.0 d	33.8 d	33.1 d	34.2 d	35.7 d	34.7 d
6	148.0 s	148.0 s	152.1 s	148.6 s	143.9 s	45.8 d	135.8 s
7	70.0 d	69.9 d	71.6 d	70.1 d	198.7 s	214.0 s	134.6 d
8	47.3 d	47.4 d	46.8 d	46.0 d	53.1 d	52.0 d	43.4 d
9	52.1 s	51.9 s	54.5 s	53.0 s	52.9 s	53.6 s	56.2 s
10	45.7 t	45.8 t	45.5 t	45.8 t	46.0 t	46.3 t	46.1 t
11	14.1 q	14.2 q	14.2 q	14.1 q	14.4 q	15.9 q	13.2 q
12	114.3 t	114.3 t	112.0 t	113.9 t	121.0 t	16.0 q	64.9 t
13	127.6 d	127.2 d	130.2 d	128.0 d	123.0 d	123.2 d	128.3 d
14	138.2 d	138.6 d	135.7 d	137.8 d	138.4 d	137.9 d	136.3 d
15	42.7 t	43.1 t	43.7 t	42.8 t	43.1 t	42.9 t	42.8 t
16	28.6 d	28.0 d	29.2 d	27.8 d	28.6 d	28.5 d	28.7 d
17	51.5 t	51.8 t	52.9 t	51.1 t	53.7 t	53.5 t	53.5 t
18	84.4 s	78.5 s	85.0 s	78.5 s	74.6 s	74.5 s	74.6 s
19	136.6 d	138.9 d	135.1 d	137.3 d	137.7 d	137.7 d	137.3 d
20	124.9 d	125.8 d	131.8 d	130.8 d	125.9 d	125.9 d	126.5 d
21	77.4 d	78.1 d	76.7 d	77.0 d	77.9 d	77.8 d	77.0 d
22	25.5 q	26.2 q	25.9 q	26.0 q	26.6 q	26.6 q	26.6 q
23	26.3 q	25.2 q	27.0 q	25.2 q	31.5 q	31.4 q	31.6 q
1′	137.5 s	137.6 s	138.9 s	137.7 s	137.0 s	137.1 s	137.7 s
2′, 6′	129.1 d	129.2 d	130.8 d	129.1 d	129.2 d	129.2 d	129.1 d
3′, 5′	129.1 d	129.1 d	129.2 d	128.9 d	129.1 d	129.1 d	129.0 d
4′	127.2 d	127.3 d	127.4 d	127.1 d	127.4 d	127.4 d	127.3 d
12-OR							170.6 s, 21.1 q
	R = Ac	R = Et	R = Ac	R = Et			
18-OR	170.1 s, 21.0 q	57.9 t, 16.3 q	170.4 s, 22.2 q	57.5 t, 16.0 q	R = H	R = H	
21-OAc	170.3 s, 22.4 q	170.3 s, 21.1 q			170.1 s, 21.1 q	170.1 s, 21.1 q	170.2 s, 21.2 q

[a] Recorded in $CDCl_3$. [b] Recorded at 100 MHz. [c] Recorded at 150 MHz. [d] Recorded in acetone-d_6. [e] Recorded at 150 MHz. [f] Recorded at 125 MHz.

18-Ethoxycytochalasin H (**2**): white solid; $[\alpha]_D^{18}$ = +39.0 (*c* 0.15, MeOH), UV (MeOH) λ_{max} (log ε): 204.0 (0.4717); ^{1}H and ^{13}C NMR data, see Tables 1 and 2; HRESIMS $[M + Na]^+$ *m*/*z* 544.3030 (calcd for $C_{32}H_{43}NO_5Na$, 544.3039).

18-Acetoxycytochalasin J (**3**): $[\alpha]_D^{22}$ = +22.0 (*c* 0.24, MeOH), UV (MeOH) λ_{max} (log ε): 204.0 (0.5467); ^{1}H and ^{13}C NMR data, see Tables 1 and 2; HRESIMS $[M + Na]^+$ *m*/*z* 516.2726 (calcd for $C_{30}H_{39}NO_5Na$, 516.2720).

18-Ethoxycytochalasin J (**4**): $[\alpha]_D^{18}$ = +50.0 (*c* 0.19, MeOH), UV (MeOH) λ_{max} (log ε): 203.8 (0.5179); ^{1}H and ^{13}C NMR data, see Tables 1 and 2; HRESIMS $[M + H]^+$ *m*/*z* 480.3111 (calcd for $C_{30}H_{42}NO_4$, 480.3108).

7-Oxocytochalasin H (**5**): $[\alpha]_D^{24}$ = −12.3 (*c* 0.19, MeOH), UV (MeOH) λ_{max} (log ε): 205.0 (0.5284); ^{1}H and ^{13}C NMR data, see Tables 1 and 2; HRESIMS $[M + Na]^+$ *m*/*z* 514.2559 (calcd for $C_{30}H_{37}NO_5Na$, 514.2564).

Cytochalasin H_3 (**6**): $[\alpha]_D^{24}$ = −63.2 (*c* 0.19, MeOH), UV (MeOH) λ_{max} (log ε): 205.5 (0.5241); ^{1}H and ^{13}C NMR data, see Tables 1 and 2; HRESIMS $[M + Na]^+$ *m*/*z* 516.2719 (calcd for $C_{30}H_{39}NO_5Na$, 516.2720).

Cytochalasin H_4 (**7**): white solid; $[\alpha]_D^{20}$ = −28.4 (*c* 0.18, MeOH), UV (MeOH) λ_{max} (log ε): 203.2 (0.5250); IR (KBr) λ_{max} 3471, 2958, 2925, 1740, 1688, 1640, 1454, 1441, 1384, 1232 cm^{-1}; ^{1}H and ^{13}C NMR data, see Tables 1 and 2; HRESIMS $[M + H]^+$ *m*/*z* 536.3014 (calcd for $C_{32}H_{42}NO_6$, 536.3007).

2.4. X-ray Crystal Structure Analysis

The intensity data for **1** and **3** were collected on a Bruker APEX DUO diffractometer using graphite-monochromated Cu Kα radiation. The structures of these compounds were solved by direct methods (SHELXS97), expanded using difference Fourier techniques, and refined by the program and full-matrix least-squares calculations. The non-hydrogen atoms were refined anisotropically, and hydrogen atoms were fixed at calculated positions. Crystallographic data for the structures of **1** (deposition number CCDC 2169670) and **3** (deposition number CCDC 2169671) have been deposited in the Cambridge Crystallographic Data Centre database. Copies of the data can be obtained free of charge from the CCDC at www.ccdc.cam.ac.uk (accessed on 1 May 2022).

Crystal data for **1**: $C_{32}H_{41}NO_6$, M = 535.66, orthorhombic, a = 9.5019 (6) Å, b = 15.8046 (9) *Å*, c = 19.6446 (11) *Å*, α = 90.00°, β = 90.00°, γ = 90.00°, V = 2950.1 (3) *Å*^{3}, T = 100 (2) K, space group P212121, Z = 4, μ (CuKα) = 0.664 mm^{-1}, 11817 reflections measured, 4764 independent reflections (R_{int} = 0.0569). The final R_1 values were 0.0917 (I > 2σ (I)). The final wR (F^2) values were 0.2549 (I > 2σ (I)). The final R_1 values were 0.0937 (all data). The final wR (F^2) values were 0.2565 (all data). The goodness of fit on F^2 was 1.163. Flack parameter = 0.3 (5). The Hooft parameter is 0.15 (11) for 1883 Bijvoet pairs.

Crystal data for **3**: $C_{30}H_{39}NO_5 \cdot H_2O$, M = 511.64, monoclinic, a = 9.7873 (3) *Å*, b = 9.4430 (3) *Å*, c = 15.5029 (4) *Å*, α = 90.00°, β = 103.6560 (10)°, γ = 90.00°, V = 1392.30 (7) *Å*^{3}, T = 100 (2) K, space group P21, Z = 2, μ (CuKα) = 0.678 mm^{-1}, 9344 reflections measured, 3802 independent reflections (R_{int} = 0.0470). The final R_1 values were 0.0600 (I > 2σ (I)). The final wR (F^2) values were 0.1736 (I > 2σ (I)). The final R_1 values were 0.0681 (all data). The final wR (F^2) values were 0.2047 (all data). The goodness of fit on F^2 was 1.093. Flack parameter = 0.1 (3). The Hooft parameter is 0.31 (9) for 1240 Bijvoet pairs.

2.5. Antimigration Assay

Cell migration was determined using the Oris™ Pro Cell Migration Assay (Platypus Technologies, Madison, WI, USA), according to the manufacturer's protocol. Briefly, MDA-MB-231 cells were seeded and incubated (37 °C, 5% CO_2) for 1 h, and then indicated concentrations of compounds were added and incubated with cells for an additional 18 h. At the end of incubation, the cell viability was evaluated with MTS assays and the migration area of each group was calculated and analysed, and the results of each subgroup were presented as a percentage of DMSO-treated cells.

3. Results and Discussion

3.1. Structure Elucidation

The molecular formula of 18-acetoxycytochalasin H (**1**) was determined to be $C_{32}H_{41}NO_6$ on the basis of HRESIMS ion at *m*/*z* 558.2826 $[M + Na]^+$ (calcd. 558.2826), indicating 13 degrees of unsaturation. Its ^{1}H NMR data (Table 1) showed typical signals of three tertiary methyl groups (δ_H 2.24, s; δ_H 2.00, s; δ_H 1.58, s), two secondary methyl groups (δ_H 0.99, d, *J* = 6.7 Hz; δ_H 1.02, d, *J* = 6.9 Hz), six olefinic protons (δ_H 5.85, dd, *J* = 16.6, 2.3 Hz; δ_H 5.74, dd, *J* = 15.5, 9.7 Hz; δ_H 5.56, d, *J* = 16.6 Hz; δ_H 5.38, m; δ_H 5.33, s; δ_H 5.10, s), two oxygenated methine groups (δ_H 5.63, d, *J* = 2.3 Hz; δ_H 3.84, d, *J* = 10.5 Hz), and one single-substituted phenyl (δ_H 7.31, t, *J* = 7.4 Hz, 2H; δ_H 7.25, t, *J* = 7.4 Hz, 1H; δ_H 7.14, d, *J* = 7.4 Hz, 2H). The ^{13}C NMR data (Table 2) displayed resonances for 32 carbons, ascribed to 5 methyls, 4 methylenes (including 1 olefinic), 11 methines (4 olefinic and 2 oxygenated), 61 quaternary carbons (1 olefinic, 1 amide and 2 ester carbonyls), and 6 other signals assignable to the single-substituted phenyl group. Thus, the above-mentioned results indicated that **1** should be a new tetracyclic cytochalasin including a benzene ring, with structural similarity with cytochalasin H [23]. The manifest difference of the structure of **1** from that of cytochalasin H was an additional acetoxy group linked at C-18 (δ_C 84.4) in **1**, which was further supported by the HMBC correlation from OAc (δ_H 2.24, s) to C-18. And the planar structure of **1** was established by extensive analysis of its 2D NMR spectra (Figure 2); its relative configuration was determined by the ROESY correlations

(Figure 3) and comparative analysis of those of cytochalasin H. Fortunately, suitable crystals of **1** were obtained and subjected to X-ray diffraction analysis using Cu Kα radiation (Figure 4), which confirmed the above deductions and unambiguously determined the absolute configuration of **1** as *3S,4R,5S,7S,8R,9R,16S,18R,21R* with the Hooft parameter 0.15 (11) for 1883 Bijvoet pairs (CCDC 2169670).

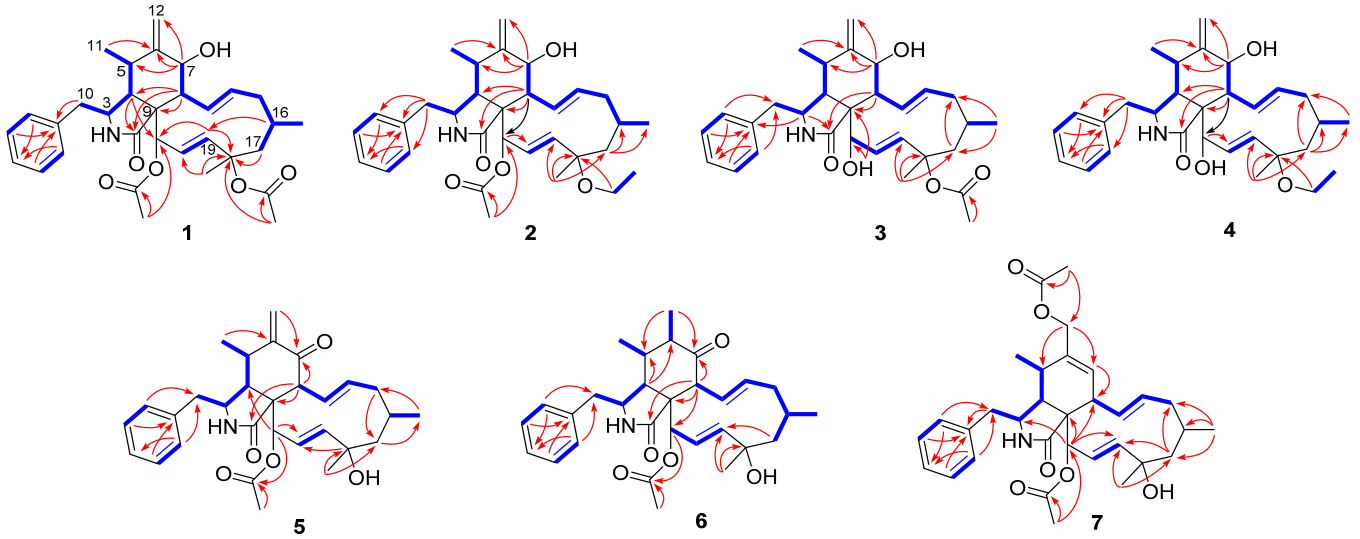

Figure 2. Key HMBC (red arrows) and ^{1}H-^{1}H COSY (blue bold) correlations of compounds **1**–**7**.

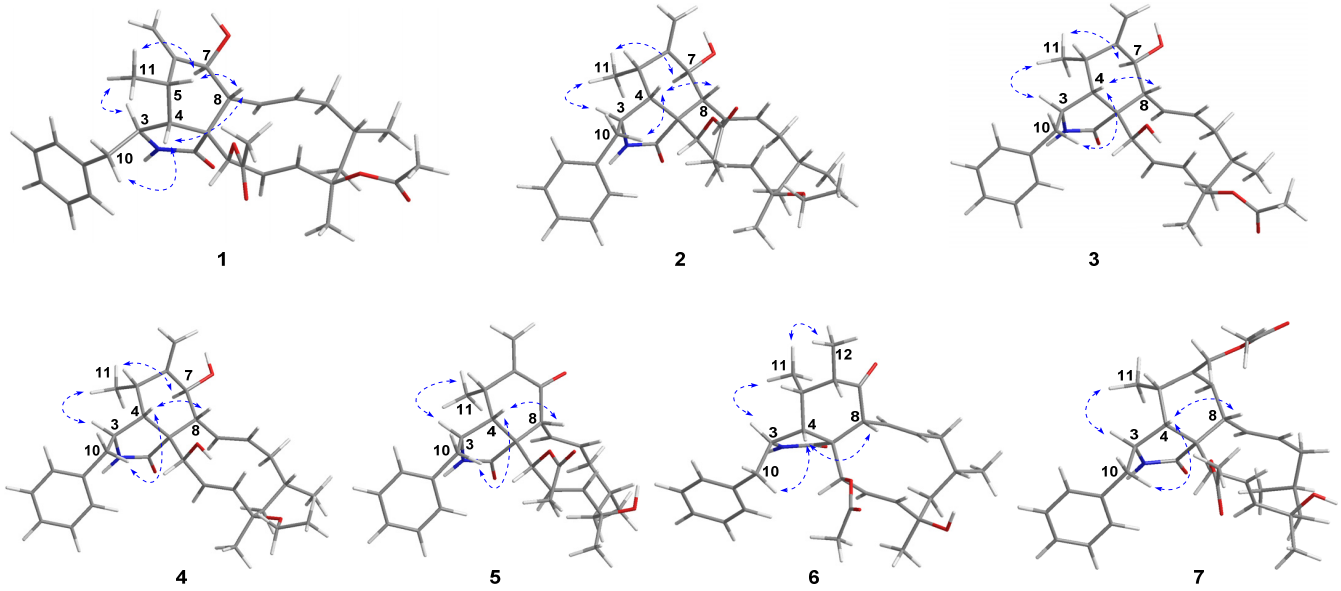

Figure 3. Key ROESY correlations of compounds **1**–**7**.

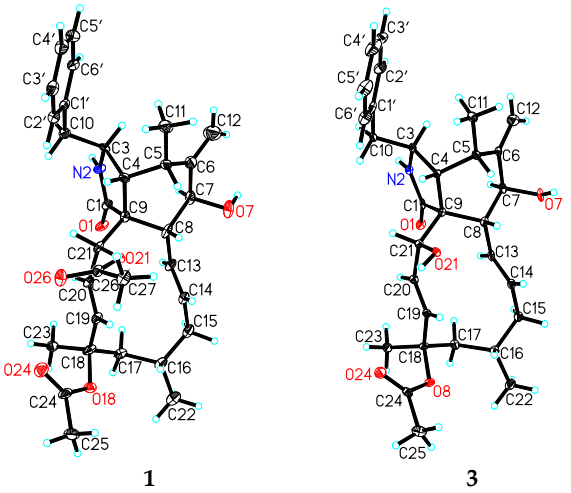

Figure 4. X-ray crystallographic structures of compounds **1** and **3**.

18-Ethoxycytochalasin H (**2**) was obtained as a white powder; its molecular formula was established as $C_{32}H_{43}NO_5$ on the basis of the HRESIMS ion peak at m/z 544.3030 $[M + Na]^+$ (calcd for $C_{32}H_{43}NO_5Na$, 544.3039), indicating 12 degrees of unsaturation. Analyses of the NMR data of **2** with those of **1** indicated their structural similarities, except for an ethoxy group located at C-18 in **2** rather than the 18-OAc group in **1**, which was confirmed by the ^1H-^1H COSY correlation of CH_2 (δ_H 3.38, m; 2.65, m)/CH_3 (1.14, t, J = 6.9 Hz) in the ethoxy group and the HMBC correlations from CH_2-18-OEt (δ_H 3.38, m; 2.65, m) to C-18 (δ_C 78.5) (Figure 2). The relative configurations of C-3, C-4, C-5, C-7, and C-8 in **2** were determined to be the same as those of **1** by analysis of the ROESY spectrum (Figure 3). Considering the almost complete consistent CD spectra of **1** and **2** (see Supplementary Materials), the absolute configuration of **2** was determined as shown.

18-Acetoxycytochalasin J (**3**) had the molecular formula of $C_{30}H_{39}NO_5$ based on the positive HRESIMS at m/z 516.2726 $[M + Na]^+$ (calcd 516.2720), corresponding to 12 degrees of unsaturation. The 1D NMR data (Tables 1 and 2) of **3** were similar to those of cytochalasin J [24], except for an additional acetoxy group located at C-18 in **3**. The above deduction was further confirmed by the changed chemical shift of C-18, compared with the ^{13}C NMR data of cytochalasin J [24], and the HMBC correlation from CH_3-18-OAc (δ_H 1.96, s) to 18-OAc carbonyl (δ_C 170.4) (Figure 2); its structure including the relative configuration was finally established as shown by X-ray diffraction analysis (Figure 4). Considering the similar CD spectra of **1** and **3** (SI), the absolute configuration of **3** was determined to be *3S,4R,5S,7S,8R,9R,16S,18R,21R*.

18-Ethoxycytochalasin J (**4**) had the molecular formula of $C_{30}H_{41}NO_4$ on the basis of the positive HRESIMS (m/z 480.3111 $[M + H]^+$, calcd 480.3108), corresponding to 11 degrees of unsaturation. Careful comparison of the ^1H and ^{13}C NMR spectra of **4** and **3** (Tables 1 and 2) suggested their similar structures, except for an ethoxy group located at C-18 in **4** rather than an acetoxy group in **3**. The above deduction was supported by the ^1H-^1H COSY correlations of CH_2/CH_3 (18-OEt) and the HMBC correlation from CH_2-18-OEt (δ_H 3.41, m; 3.37, m) to C-18 (δ_C 78.5) (Figure 2). The absolute configuration of **4** was determined to be the same as that of **1** by analysis of their CD spectra; thus, the structure of **4** was established as shown (Figure 1).

7-Oxocytochalasin H (**5**) possessed the molecular formula of $C_{30}H_{37}NO_5$ with 13 degrees of unsaturation, which was determined by the positive HRESIMS (m/z 514.2559 $[M + Na]^+$, calcd 514.2564). Analysis of the ^1H and ^{13} C NMR data (Tables 1 and 2) of **5** and cytochalasin H [23] indicated their structural similarity. The manifest differences were that the C-7 oxymethine group in cytochalasin H was replaced by the C-7 carbonyl group (δ_C 198.7) in **5**. The HMBC correlations from H-8 (δ_H 3.94, d, J = 9.3 Hz) and H_2-12 (δ_H 6.25, s) to C-7 and other correlations in the 2D spectra of **5** confirmed the above deduction (Figure 2).

The correlations of H-4/H-8, H_2-10/H-4, and H_3-11/H-3 in the ROESY spectrum indicated that H-3 was *a*-oriented and H-4, H-5, H-8 were *β*-oriented (Figure 3). Considering the same biogenetic pathway of **1** and **5**, the structure of **5** was determined as shown (Figure 1).

Cytochalasin H_3 (**6**) had the molecular formula of $C_{30}H_{39}NO_5$ with 12 degrees of unsaturation, which was determined by the positive HRESIMS (*m*/*z* 516.2719 $[M + Na]^+$, calcd 516.2720). Detailed analysis of ^1H and ^{13}C NMR data of **6** (Tables 1 and 2) indicated that **6** possessed a similar structure to that of **5**, except for the presence of a saturated C–C bond between C-6 (δ_C 45.8) and C-12 (δ_C 16.0) in **6** rather than a terminal double bond in **5**, which was further confirmed by the ^1H–^1H COSY correlation of H-6/H_3-12 and the HMBC correlations from H_3-12 (δ_H 1.12, d, *J* = 7.0 Hz) to C-5 (δ_C 35.7) and C-7 (δ_C 214.0) (Figure 2). The ROESY correlations of H-3/H_3-11, H_3-11/H_3-12, H_2-10/H-4, and H-4/H-8 implied the *α*-orientation of H-3 and *β*-orientations of H-4, H-5, H-6, and H-8 (Figure 3). By analysis of the similar CD spectra of **6** and **1** and biogenetic consideration, the structure of **6** was determined as shown.

The molecular formula of cytochalasin H_4 (**7**) was deduced to be $C_{32}H_{41}NO_6$ with 13 degrees of unsaturation based on the positive HRESIMS (*m*/*z* 536.3014 $[M + H]^+$, calcd 536.3007). The ^{13}C NMR data (Tables 1 and 2 of **7** displayed resonances for 32 carbons, ascribed to five methyls, four methylenes (including one oxygenated), 11 methines (5 olefinic and one oxygenated), six quaternary carbons (one olefinic, one amide and two ester carbonyls), and 6 other signals assignable to the single-substituted phenyl group. The above-mentioned results indicated the presence of an additional acetoxy group and an oxymethine group compared to those of the known RKS-1778 (**10**) [25]. The ROESY correlations of H-3/H_3-11, H_2-10/H-4, and H-4/H-8 implied the *α*-orientation of H-3 and *β*-orientations of H-4, H-5, and H-8 (Figure 3). The absolute configuration of **7** was determined as shown by analysis of their similar CD spectra of **7** and **10** and biogenetic consideration.

Compounds **8**–**11** were identified as cytochalasin H (**8**) [23], cytochalasin J_1 (**9**) [24], RKS-1778 (**10**) [25], 21-acetoxycytochalasin J_2 (**11**) [26] on the basis of their spectroscopic features and by comparison with the published data in the literature. Biogenetically, compounds **1**–**11** might be derived from a polyketide chain (octaketide) and an amino acid building block (phenylalanine) through a number of steps involving cycloaddition, oxidation, reduction, dehydration, acetylation, ethylation and methylation [27,28].

3.2. Antimigratory Activity

Our previous studies have revealed that phomopchalasins B and C displayed antimigratory effects [19]. In order to explore the potential of the cytochalasans on antimigration against tumours, eight compounds in sufficient natural amounts (Table 3) were evaluated for antimigratory activities against MDA-MB-231 in vitro. As a result, **1**–**3** and **8**–**11** exhibited in vitro antimigratory effects with IC_{50} values in the range of 1.01–10.42 μM (cytochalasin D as the positive control); it suggested the activity decreased when the C-18 hydroxy group was substituted with the acetoxy, ethoxy or methoxy group (**8** vs. **1**, **2**, and **9**). When a double bond was introduced between C-17 and C-18 rather than an ethoxy or methoxy group at C-18, the activity slightly improved (**11** vs. **2** and **9**). Compound **3** displayed antimigratory activity with an IC_{50} value of 6.38 μM. The introduction of an acetoxy group at C-21 may enhance the activity (**1** vs. **3**). When the unit of a terminal double bond (C6-C12) and a hydroxy group at C-7 was replaced by a trisubstituted alkene (C12-C6-C7), the activity slightly improved (**8** vs. **10**), but the further introduction of an acetoxy group at C-12 decreased the activity (**10** vs. **7**).

Table 3. Antimigratory activities of the compounds against MDA-MB-231 in vitro.

Compounds	IC_{50} (μM)	Compounds	IC_{50} (μM)
Cytochalasin D [a]	0.78	**8**	1.25
1	3.14	**9**	7.31
2	10.42	**10**	1.01
3	6.38	**11**	6.41
7	>25		

[a] Positive control.

4. Conclusions

Seven new cytochalasans (**1**–**7**), together with four known ones, cytochalasin H (**8**), cytochalasin J_1 (**9**), RKS-1778 (**10**), and 21-acetoxycytochalasin J_2 (**11**), were isolated from *Phomopsis* sp. shj2. Their structures were elucidated through extensive spectroscopic data interpretation and single-crystal X-ray diffraction analysis. In the present study, eight cytochalasans were evaluated for their antimigratory activity. Compounds **1**–**3** and **8**–**11** exhibited antimigratory activity against MDA-MB-231 in vitro with IC_{50} values in the range of 1.01−10.42 μM. The results will lay a foundation for further study of the structure–activity relationship for the discovery of antitumour lead compounds.

Supplementary Materials: The following supporting information can be downloaded at: https://www.mdpi.com/article/10.3390/jof8050543/s1, Section S1: NMR, HRESIMS, UV, ORD, and CD spectra of compound **1**; Section S2: NMR, HRESIMS, UV, ORD, and CD spectra of compound **2**; Section S3: NMR, HRESIMS, UV, ORD, and CD spectra of compound **3**; Section S4: NMR, HRESIMS, UV, ORD, and CD spectra of compound **4**; Section S5: NMR, HRESIMS, UV, ORD, and CD spectra of compound **5**; Section S6: NMR, HRESIMS, UV, ORD, and CD spectra of compound **6**; Section S7: NMR, HRESIMS, UV, ORD, and CD spectra of compound **7**.

Author Contributions: Conceptualization, B.-C.Y. and P.-T.P.; methodology, W.-G.W., B.-C.Y., L.-M.K., J.-W.T., X.D., Y.L. and P.-T.P.; resources, W.-G.W., B.-C.Y., Y.L. and P.-T.P.; data curation, B.-C.Y. and L.-M.K.; writing—original draft preparation, B.-C.Y.; writing—review and editing, B.-CY. and P.-T.P.; project administration, B.-C.Y. and P.-T.P.; funding acquisition, B.-C.Y. and P.-T.P. All authors have read and agreed to the published version of the manuscript.

Funding: This research was funded by the National Natural Science Foundation of China (No. 81874298), the NSFC-Joint Foundation of Yunnan Province (U2002221), and the Yunnan Science Fund for Distinguished Young Scholars (2019FJ002), and the Postdoctoral Directional Training Foundation of Yunnan Province (B.-C.Y.).

Institutional Review Board Statement: Not applicable.

Data Availability Statement: X-ray crystallographic data of **1** and **3** (CIF) are available free of charge from the CCDC at https://www.ccdc.cam.ac.uk (accessed on 1 May 2022).

Conflicts of Interest: The authors declare no conflict of interest.

References

1. Rai, N.; Keshri, P.K.; Verma, A.; Kamble, S.C.; Mishra, P.; Barik, S.; Singh, S.K.; Gautam, V. Plant associated fungal endophytes as a source of natural bioactive compounds. *Mycology* **2021**, *12*, 139–159. [CrossRef] [PubMed]
2. Deshmukh, S.K.; Dufossé, L.; Chhipa, H.; Saxena, S.; Mahajan, G.B.; Gupta, M.K. Fungal endophytes: A potential source of antibacterial compounds. *J. Fungi* **2022**, *8*, 164. [CrossRef] [PubMed]
3. Xiao, Y.; Liang, W.; Zhang, Z.; Wang, Y.; Zhang, S.; Liu, J.; Chang, J.; Ji, C.; Zhu, D. Polyketide derivatives from the endophytic fungus *Phaeosphaeria* sp. LF5 isolated from *Huperzia serrata* and their acetylcholinesterase inhibitory activities. *J. Fungi.* **2022**, *8*, 232. [CrossRef] [PubMed]
4. Chen, Y.; Yang, W.; Zou, G.; Wang, G.; Kang, W.; Yuan, J.; She, Z. Cytotoxic bromine- and iodine-containing cytochalasins produced by the mangrove endophytic fungus *Phomopsis* sp. QYM-13 using the OSMAC approach. *J. Nat. Prod.* **2022**. [CrossRef]
5. Miao, S.; Liu, M.; Qi, S.; Wu, Y.; Sun, K.; Zhang, Z.; Zhu, K.; Cai, G.; Gong, K. Cytochalasins from coastal saline soil-derived fungus *Aspergillus flavipes* RD-13 and their cytotoxicities. *J. Antibiot.* **2022**. [CrossRef]
6. Zhang, J.-Y.; He, J.; Li, Z.-H.; Feng, T.; Liu, J.-K. Zopfiellasins A–D, two pairs of epimeric cytochalasins from kiwi-associated fungus *Zopfiella* sp. and their antibacterial assessment. *Molecules* **2021**, *26*, 5611. [CrossRef]

7. Zhang, X.; Wu, Z.; Bao, A.; Zhao, Z.; Chen, Y.; Zhao, H.; Wang, J.; Chen, C.; Tong, Q.; Zhu, H.; et al. Asperflavipines C–E and aspermichalasine A: Three cytochalasan heterotetramers and an unusual cytochalasan monomer from *Aspergillus micronesiensis*. *Org. Chem. Front.* **2022**, *9*, 2585–2592. [CrossRef]
8. Yang, X.; Wu, P.; Xue, J.; Li, H.; Wei, X. Cytochalasans from endophytic fungus *Diaporthe* sp. SC-J0138. *Fitoterapia* **2020**, *145*, 104611. [CrossRef]
9. Long, X.; Wu, H.; Ding, Y.; Qu, C.; Deng, J. Biosynthetically inspired divergent syntheses of merocytochalasans. *Chem* **2021**, *7*, 212–223. [CrossRef]
10. Bao, R.; Tian, C.; Zhang, H.; Wang, Z.; Dong, Z.; Li, Y.; Gao, M.; Zhang, H.; Liu, G.; Tang, Y. Total syntheses of asperchalasines A–E. *Angew. Chem. Int. Ed.* **2018**, *57*, 14216–14220. [CrossRef]
11. Hua, C.; Yang, Y.; Sun, L.; Dou, H.; Tan, R.; Hou, Y. Chaetoglobosin F, a small molecule compound, possesses immunomodulatory properties on bone marrow-derived dendritic cells via TLR9 signaling pathway. *Immunobiology* **2013**, *218*, 292–302. [CrossRef] [PubMed]
12. Ye, K.; Ai, H.-L.; Liu, J.-K. Identification and bioactivities of secondary metabolites derived from endophytic fungi isolated from ethnomedicinal plants of Tujia in Hubei Province: A review. *Nat. Prod. Bioprospect.* **2021**, *11*, 185–205. [CrossRef] [PubMed]
13. Zheng, Q.-C.; Kong, M.-Z.; Zhao, Q.; Chen, G.-D.; Tian, H.-Y.; Li, X.-X.; Guo, L.-D.; Li, J.; Zheng, Y.-Z.; Gao, H. Chaetoglobosin Y, a new cytochalasan from *Chaetomium globosum*. *Fitoterapia* **2014**, *93*, 126–131. [CrossRef]
14. Evidente, A.; Andolfi, A.; Vurro, M.; Zonno, M.C.; Motta, A. Cytochalasins Z4, Z5, and Z6, three new 24-oxa[14]cytochalasans produced by *Phoma exigua* var. *heteromorpha*. *J. Nat. Prod.* **2003**, *66*, 1540–1544. [CrossRef] [PubMed]
15. Gupta, G.P.; Massagué, J. Cancer metastasis: Building a framework. *Cell* **2006**, *127*, 679–695. [CrossRef]
16. Nakashima, K.; Tomida, J.; Kamiya, T.; Hirai, T.; Morita, Y.; Hara, H.; Kawamura, Y.; Adachi, T.; Inoue, M. Diaporthols A and B: Bioactive diphenyl ether derivatives from an endophytic fungus *Diaporthe* sp. *Tetrahedron Lett.* **2018**, *59*, 1212–1215. [CrossRef]
17. Yahagi, H.; Yahagi, T.; Furukawa, M.; Matsuzaki, K. Antiproliferative and antimigration activities of beauvericin isolated from *Isaria* sp. on pancreatic cancer cells. *Molecules* **2020**, *25*, 4586. [CrossRef]
18. Monteillier, A.; Allard, P.-M.; Gindro, K.; Wolfender, J.-L.; Cuendet, M. Lung cancer chemopreventive activity of patulin isolated from *Penicillium vulpinum*. *Molecules* **2018**, *23*, 636. [CrossRef]
19. Yan, B.-C.; Wang, W.-G.; Hu, D.-B.; Sun, X.; Kong, L.-M.; Li, X.-N.; Du, X.; Luo, S.-H.; Liu, Y.; Li, Y.; et al. Phomopchalasins A and B, two cytochalasans with polycyclic-fused skeletons from the endophytic fungus *Phomopsis* sp. shj2. *Org. Lett.* **2016**, *18*, 1108–1111. [CrossRef]
20. Tang, J.-W.; Kong, L.-M.; Zu, W.-Y.; Hu, K.; Li, X.-N.; Yan, B.-C.; Wang, W.-G.; Sun, H.-D.; Puno, P.-T. Isopenicins A–C: Two types of antitumor meroterpenoids from the plant endophytic fungus *Penicillium* sp. sh18. *Org. Lett.* **2019**, *21*, 771–775. [CrossRef]
21. Xia, J.-N.; Hu, K.; Su, X.-Z.; Tang, J.-W.; Li, X.-N.; Sun, H.-D.; Puno, P.-T. Discovery of *ent*-kaurane diterpenoids, characteristic metabolites of *Isodon* species, from an endophytic fungal strain *Geopyxis* sp. XY93 inhabiting *Isodon parvifolia*. *Fitoterapia* **2022**, *158*, 105160. [CrossRef] [PubMed]
22. Su, X.-Z.; Zhu, Y.-Y.; Tang, J.-W.; Hu, K.; Li, X.-N.; Sun, H.-D.; Li, Y.; Puno, P.-T. Pestaloamides A and B, two spiro-heterocyclic alkaloid epimers from the plant endophytic fungus *Pestalotiopsis* sp. HS30. *Sci. China Chem.* **2020**, *63*, 1208–1213. [CrossRef]
23. Izawa, Y.; Hirose, T.; Shimizu, T.; Koyama, K.; Natori, S. Six new 10-pheynl-[11]cytochalasans, cytochalasins N–S from *Phomopsis* sp. *Tetrahedron* **1989**, *45*, 2323–2335. [CrossRef]
24. Shang, Z.; Raju, R.; Salim, A.A.; Khalil, Z.G.; Capon, R.J. Cytochalasins from an Australian marine sediment-derived *Phomopsis* sp. (CMB-M0042F): Acid-mediated intramolecular cycloadditions enhance chemical diversity. *J. Org. Chem.* **2017**, *82*, 9704–9709. [CrossRef] [PubMed]
25. Kakeya, H.; Morishita, M.; Onozawa, C.; Usami, R.; Horikoshi, K.; Kimura, K.; Yoshihama, M.; Osada, H. RKS-1778, a new mammalian cell-cycle inhibitor and a key intermediate of the [11] cytochalasin group. *J. Nat. Prod.* **1997**, *60*, 669–672. [CrossRef]
26. Huang, X.; Zhou, D.; Liang, Y.; Liu, X.; Cao, F.; Qin, Y.; Mo, T.; Xu, Z.; Li, J.; Yang, R. Cytochalasins from endophytic *Diaporthe* sp. GDG-118. *Nat. Prod. Res.* **2021**, *35*, 3396–3403. [CrossRef]
27. Scherlach, K.; Boettger, D.; Remme, N.; Hertweck, C. The chemistry and biology of cytochalasans. *Nat. Prod. Rep.* **2010**, *27*, 869–886. [CrossRef]
28. Qiao, K.; Chooi, Y.-H.; Tang, Y. Identification and engineering of the cytochalasin gene cluster from *Aspergillus clavatus* NRRL 1. *Metab. Eng.* **2011**, *13*, 723–732. [CrossRef]